



Unique biomechanical signatures of Bryan, Prodisc C, and Prestige LP cervical disc replacements: a finite element modelling study

Hoon Choi¹ · Yuvaraj Purushothaman^{1,2} · Jamie Baisden¹ · Narayan Yoganandan¹

Received: 24 April 2019 / Revised: 26 July 2019 / Accepted: 12 August 2019 / Published online: 12 October 2019

© This is a U.S. government work and its text is not subject to copyright protection in the United States; however, its text may be subject to foreign copyright protection 2019

Abstract

Purpose The purpose of the study is to examine the biomechanical alterations in the index and adjacent levels of the human cervical spine after cervical arthroplasty with Bryan, Prodisc C, or Prestige LP.

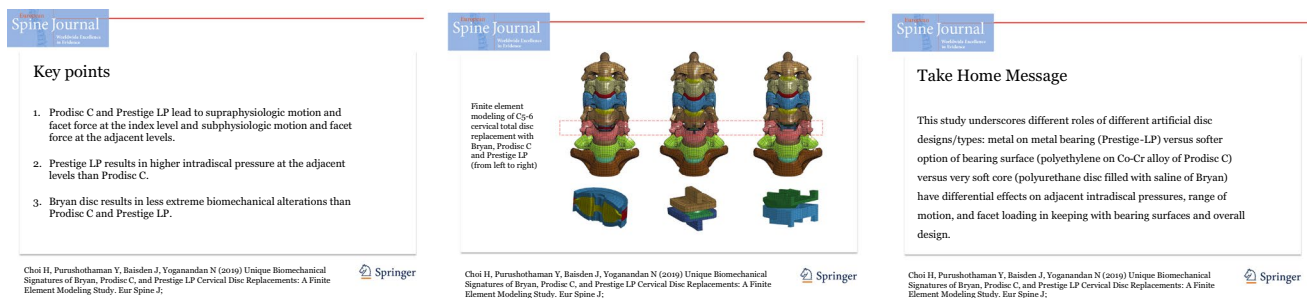
Methods A previously validated C2–T1 osteoligamentous finite element model was used to perform virtual C5–6 arthroplasty using three different FDA-approved artificial cervical discs. Motion-controlled moment loading protocol was used. Moment was varied until Bryan, Prodisc C, and Prestige LP models displayed the same total range of motion across C3–C7 as the intact spine model at 2 Nm of pure moment loading. Range of motion (ROM) and facet force (FF) were recorded at the index level. ROM, FF, and intradiscal pressure (IDP) were recorded at the adjacent levels.

Results Prodisc C and Prestige LP led to supraphysiologic ROM and FF at the index level while decreasing ROM and FF at the adjacent levels. In contrast, Bryan reduced ROM and FF at the index level. Bryan increased ROM and FF at the adjacent levels in flexion, but decreased ROM and FF in the adjacent levels in extension. Prodisc C decreased IDP at the adjacent levels. Bryan reduced IDP in extension only. Prestige LP increased adjacent-level IDP.

Conclusions The distinct designs and material compositions of the three artificial discs result in varying biomechanical alterations at the index and adjacent levels in the cervical spine after implantation. The findings confirm the design and material influence on the spine biomechanics, as well as the advantages and contraindications of cervical arthroplasty in general.

Graphic abstract

These slides can be retrieved under Electronic Supplementary Material.



Keywords Cervical artificial disc · Cervical arthroplasty · Cervical total disc replacement · Finite element modelling · Biomedical engineering

Electronic supplementary material The online version of this article (<https://doi.org/10.1007/s00586-019-06113-y>) contains supplementary material, which is available to authorized users.

✉ Hoon Choi
hchoi@mcw.edu

Extended author information available on the last page of the article

Abbreviations

| | |
|------|---|
| ACDF | Anterior cervical discectomy and fusion |
| ROM | Range of motion |
| IDP | Intradiscal pressure |
| FF | Facet force |
| FEM | Finite element modeling |

Introduction

Many artificial discs are available for cervical spine arthroplasty although all are not approved by the Food and Drug Administration (FDA) in the USA [1]. Not all artificial disc designs will behave the same mechanically because of the distinctiveness of each implant design [2–13]. Disc designs vary widely in terms of translation of the axis of rotation (constrained versus unconstrained), range of motion (flexion/extension, rotation and lateral bending), materials (titanium, hydroxyapatite coating, cobalt–chromium alloy, ultra-high molecular weight polyethylene, and polyurethane), number of moving pieces, and encapsulation of the overall design (open versus closed). While design features are distinct, the end goal is to render the spine to have motion at the index level, thus limiting the motions at the adjacent levels [1, 14–16]. Affected biomechanical variables include the range of motion (ROM), intradiscal pressure (IDP), and facet loads. With the prospect of more designs, a predictable model that can evaluate same-level facet pressures, ROM, and adjacent-level IDPs will be of value to the clinician. The present study is designed with this objective.

Regarding the materials used in the design of the artificial discs, while all materials are intended to provide a bearing that is flexible to allow the range of motion at the index level, the varying surface characteristics from the implant are expected to impart differing vertebral body–artificial disc–vertebral body mechanical interface characteristics, and the design also plays a role. The fixation of the disc with the adjacent bones is also different.

Prestige LP is an open two-piece, semi-constrained design with metal-on-metal articulation. Prodisc C is an open two-piece, semi-constrained design with polymer-on-metal articulation. Bryan is a closed one-piece, unconstrained (no fixed core or centre of rotation) design with a saline-lubricated polyurethane core. The present study is designed to compare the biomechanical alterations after cervical arthroplasty with Bryan, Prodisc C, and Prestige LP using an anatomically accurate model of the entire cervical spinal column that has been validated under different loading environments.

Finite element analysis (FEA) has been used to evaluate joint prosthesis, and this includes the lumbar spine and hip joint. Such FEA models have prescribed profiles for axial compression and cyclic motion in three planes for disc devices [17–19]. Questioning the clinical relevance of such models, FEAs with ADR placed in the spine (ADR-spine) were shown to be superior to the earlier models [20]. In the cited study, the authors showed that the ADR-spine FEM predicted localized wear in certain regions, while the uniformly distributed wear pattern was shown

in the ADR-only FEM. Furthermore, the cumulative volumetric wear for the ADR-only model was ten times that of the ADR-spine model. The ADR-spine FEM also revealed a separation at the articulating interface during extension and lateral bending. Such phenomenon compared well with clinical observations, especially in hip arthroplasty. From these perspectives, while the present paper does not cover all the aspects of evaluating the joint prosthesis, FEM has evolved in the cervical spine for ADR surgeries.

With a focus on the cervical spine, anterior cervical discectomy and fusion (ACDF) is one of the most commonly performed operations in the world for degeneration of the cervical spine. It is indicated for symptomatic cervical radiculopathy and/or myelopathy that is unresponsive to non-surgical management. C5/6 is the most commonly operated level [21]. After ACDF, adjacent segment degeneration can occur. This may be due to potentially increased stress at the adjacent levels, sometimes leading to surgery and extension of the previous fusion construct. Cervical arthroplasty is an alternative to ACDF that consists of implanting an artificial disc in the disc space after discectomy. Cervical arthroplasty is a motion-preserving strategy that could theoretically maintain motion at the index segment and decrease stress at the adjacent segments, thereby reducing the chance of adjacent segment degeneration. There is a paucity of studies directly comparing the biomechanical alterations of various commercially available cervical artificial discs. Finite element analysis can provide information that is otherwise unobtainable or impractical to obtain from human clinical studies. Some examples include intradiscal pressure, facet force, and range of motion at each segment of the cervical spine. Another advantage of finite element modelling (FEM) is the elimination of confounding factors by keeping the cervical spine morphology and characteristics identical across different study groups except for the study variables.

Specifically, the goal of this study was to evaluate and compare the biomechanical alterations at the index and adjacent levels after total cervical disc replacement using three different implants.

Methods

A previously published C2–T1 osteoligamentous model (Fig. 1) was used for the study [22–25]. The intact spinal model was validated for range of motion (ROM), intradiscal pressure (IDP), and facet force (FF) based on values from the literature [26–28]. The model consisted of seven segments (C2–T1) meshed with hexahedral element with materials properties obtained from the literature [22–25]. The model contained intervertebral disc, anterior longitudinal ligament (ALL), posterior longitudinal ligament (PLL), capsular ligaments (CL), ligamentum flavum (LF),

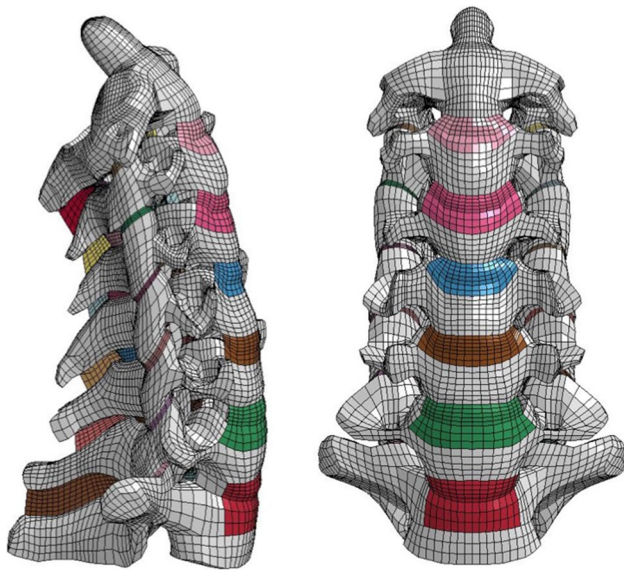


Fig. 1 C2-T1 osteoligamentous finite element model

and interspinous ligaments (ISL). The intervertebral disc was modelled as two distinct regions: annulus fibrosus and nucleus pulposus. The annulus consisted of the ground substance and fibre definitions. The anterior region of the annulus fibrosus consisted of eight-pair layers (total in 16), and the posterior region consisted of four layers (total in 8). The anterior annulus fibres did not form a continuous ring with the posterior annulus fibres, forming a gap bilaterally at the uncovertebral clefts [29]. There were total of 11,452 elements in the entire model for the annulus fibres.

The number of elements on each level at from the C2–C3 to C7–T1 levels was 1392, 2060, 1970, 2060, 2130, and 1840, respectively. The hyper-elastic foam ground substance was defined using the Hill strain energy function. The fibres were defined using membrane elements with tension-only directional fibres embedded in the ground substance. The fibres in the anterior annulus region were defined in a crisscross manner, while fibres in the posterior region were defined in the vertical direction [23, 30, 31]. The C2–T1 finite element model was modified at the C5/6 functional spine unit to simulate cervical arthroplasty. Discectomy was performed, and ALL and PLL were both removed prior to artificial disc insertion.

Prodisc C (Centinel Spine, West Chester, PA, USA), Bryan (Medtronic Sofamor Danek, Memphis, TN, USA), and Prestige LP (Medtronic Sofamor Danek, Memphis, TN, USA) were modelled using actual specimens and material properties available in the literature (Table 1). Implant size selection and placement in the vertebral segments were done as per the standard surgical technique. The Prodisc C model consisted of two cobalt chrome alloy endplates and a core made of ultra-high molecular weight polyethylene (Fig. 2). The Bryan disc model consisted of upper and lower titanium endplates connected by a polyurethane membrane containing a saline-lubricated polyurethane core. The surface-to-surface contact was applied between the moving segments of the discs, and a tied contact condition was defined at the bone–implant interface. The Prestige LP model consisted of two titanium carbide endplates with the upside-down dome of superior endplate articulating with the groove of the inferior endplate.

Fig. 2 Finite element modeling of C5-6 cervical total disc replacement with Bryan, Prodisc C and Prestige LP (from left to right)

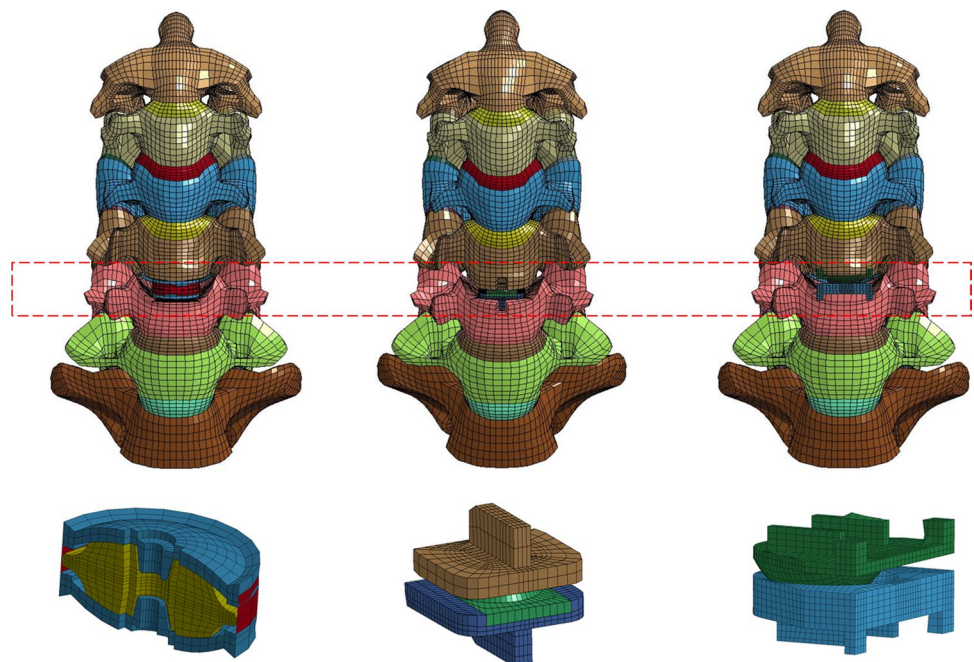


Table 1 Finite element modelling characteristics of the three cervical artificial discs

| Disc types | No. of elements | Element type | Material type | Material properties |
|-------------------------|-----------------|------------------------------|--|--------------------------------|
| Prodisc C [15] | | | | |
| Top plate | 880 | Eight-noded hexahedral solid | Cobalt–chromium–molybdenum alloy | $E = 220$ Gpa $\mu = 0.32$ |
| Core | 2048 | Eight-noded hexahedral solid | Ultra-high molecular weight polyethylene | $E = 2$ Gpa $\mu = 0.27$ |
| Bottom plate | 1108 | Eight-noded hexahedral solid | Cobalt–chromium–molybdenum alloy | $E = 220$ Gpa $\mu = 0.32$ |
| Bryan [18] | | | | |
| Outer shell | 1104 | Eight-noded hexahedral solid | Titanium | $E = 110$ Gpa $\mu = 0.3$ |
| Nucleus | 2688 | Eight-noded hexahedral solid | Polyurethane | $E = 0.03$ Gpa $\mu = 0.45$ |
| Sheath | 144 | Four-noded quad membrane | Titanium | $E = 110$ Gpa $\mu = 0.3$ |
| Prestige LP [20] | | | | |
| Upper part (ball) | 2020 | Eight-noded hexahedral solid | Titanium carbide | $E = 110$ Gpa $\mu = 0.3$ |
| Lower part (trough) | 4086 | Eight-noded hexahedral solid | Titanium carbide | $E = 110$ Gpa $\mu = 0.3$ |

All the finite element models were fixed at the T1 vertebra for all degrees of freedom, and the load was applied at the superior endplate of C2. Pure moment loading with 2 Nm for flexion and extension was applied to the intact spine. ROM between C3 and C7 was measured.

This was accomplished using the hybrid loading protocol [32]. Briefly, the protocol in its original form consists of: (a) applying pure moments to intact spine, (b) applying pure moments to implanted spine until its ROM equals that of the intact spine, i.e. results from previous step, and (c) statistical comparison of the biomechanical variables between the two conditions. Step (a) was described earlier. For step (b), the moment was applied to the Bryan, Prodisc C, and Prestige LP models until the ROM between C3 and C7 matched with the results found for the intact spine model under 2 Nm of loading. Step (c) was not carried out as this was a finite element model-based study, and it should be noted that the original protocol consisting of the various steps was specified for human cadaver spine experiments. This motion-controlled moment loading [3, 7, 32, 33] was chosen to simulate the clinical setting where the total motion of the cervical spine is of relevance. ROM and FF were measured at the index level. ROM, IDP, and FF were recorded at the rostral and caudal adjacent levels.

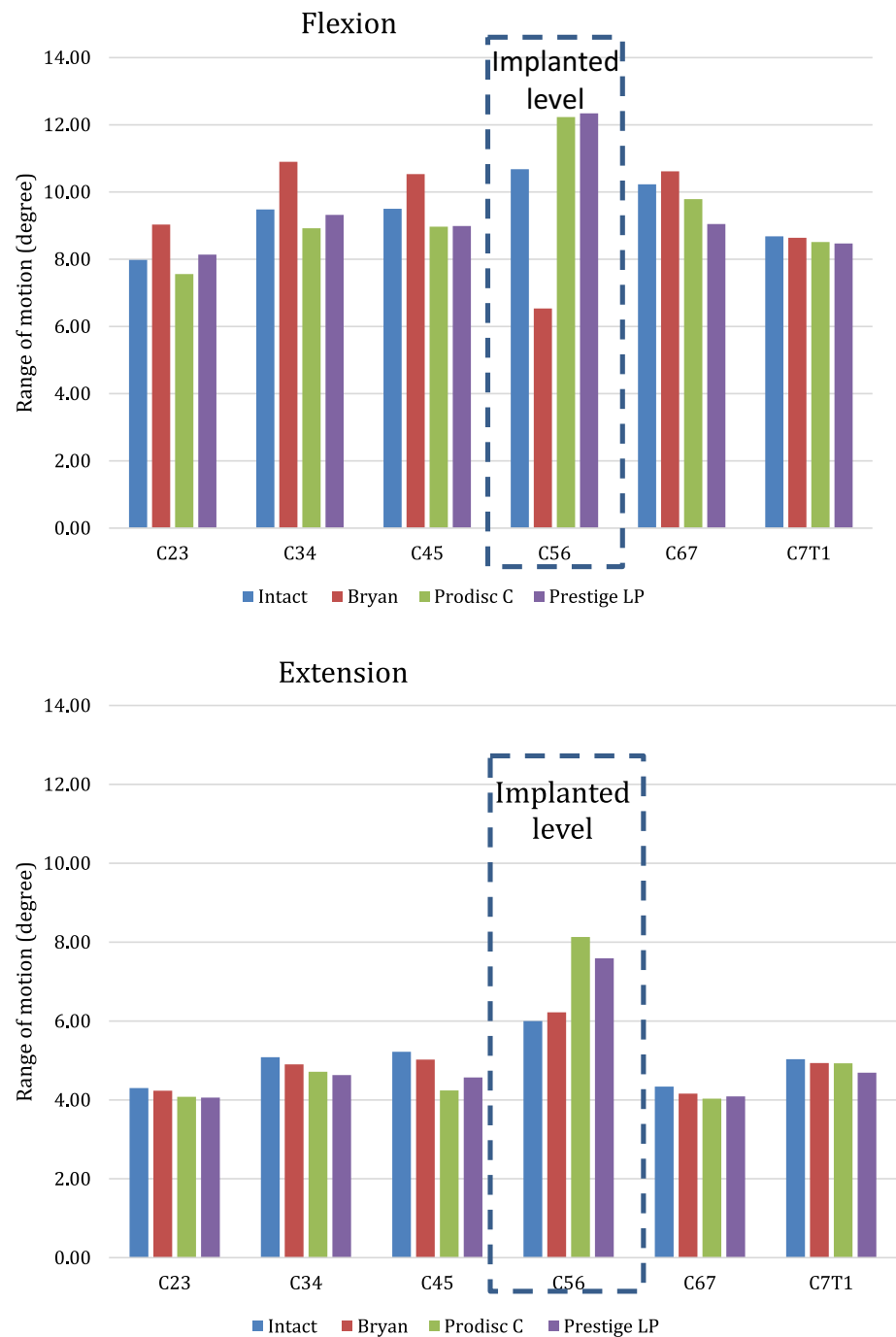
Results

Moments required to achieve the same range of motion across C3–7 as the intact model at 2 Nm were as follows: Bryan (2.6 Nm for flexion and 1.9 Nm for extension),

Prodisc C (1.8 Nm for flexion and 1.4 Nm for extension), and Prestige LP (2.2 Nm for flexion and 2.1 for extension). Bryan reduced flexion by 38.81% but increased extension by 0.04% in the index level (Fig. 3). It increased flexion by 10.87% and 3.78% at C4/5 and C6/7, respectively, while decreasing extension by 0.04% at C4/5 and C6/7. Prodisc C and Prestige LP both increased ROM at the index level while reducing ROM at the adjacent levels. Prodisc C increased flexion by 14.51% and extension by 35.5% at C5/6 while reducing flexion by 5.57% and extension by 18.77% at C4/5 and flexion and extension by 4.3% and 7.05%, respectively, at C6/7. Prestige LP increased flexion by 15.54% and extension by 26.5% at the index level. C4/5 and C6/7 showed reduced flexion (by 5.37% and 11.53%) and extension (by 12.45% and 5.71%, respectively).

Bryan reduced facet force at the index facets (by 20% in flexion and 59% in extension) (Fig. 4). It increased facet force by 28.52% at C4/5 and 1.02% at C6/7 in flexion, but reduced facet force by 4.88% at C4/5 and 13.54% at C6/7 in extension. Prodisc C increased facet force at the index level by 33.96% in flexion and by 181.44% in extension. It reduced facet force at the adjacent levels in both flexion (by 22.9% at C4/5 and 17.47% at C6/7) and extension (by 17.89% at C4/5 and 23.2% at C6/7). Prestige LP increased facet force by 77.17% in flexion and by 209.68% in extension at the index level, while reducing adjacent segment facet forces in both flexion (by 11.16% at C4/5 and 12.64% at C6/7) and extension (by 12.94% at C4/5 and 18.8% at C6/7).

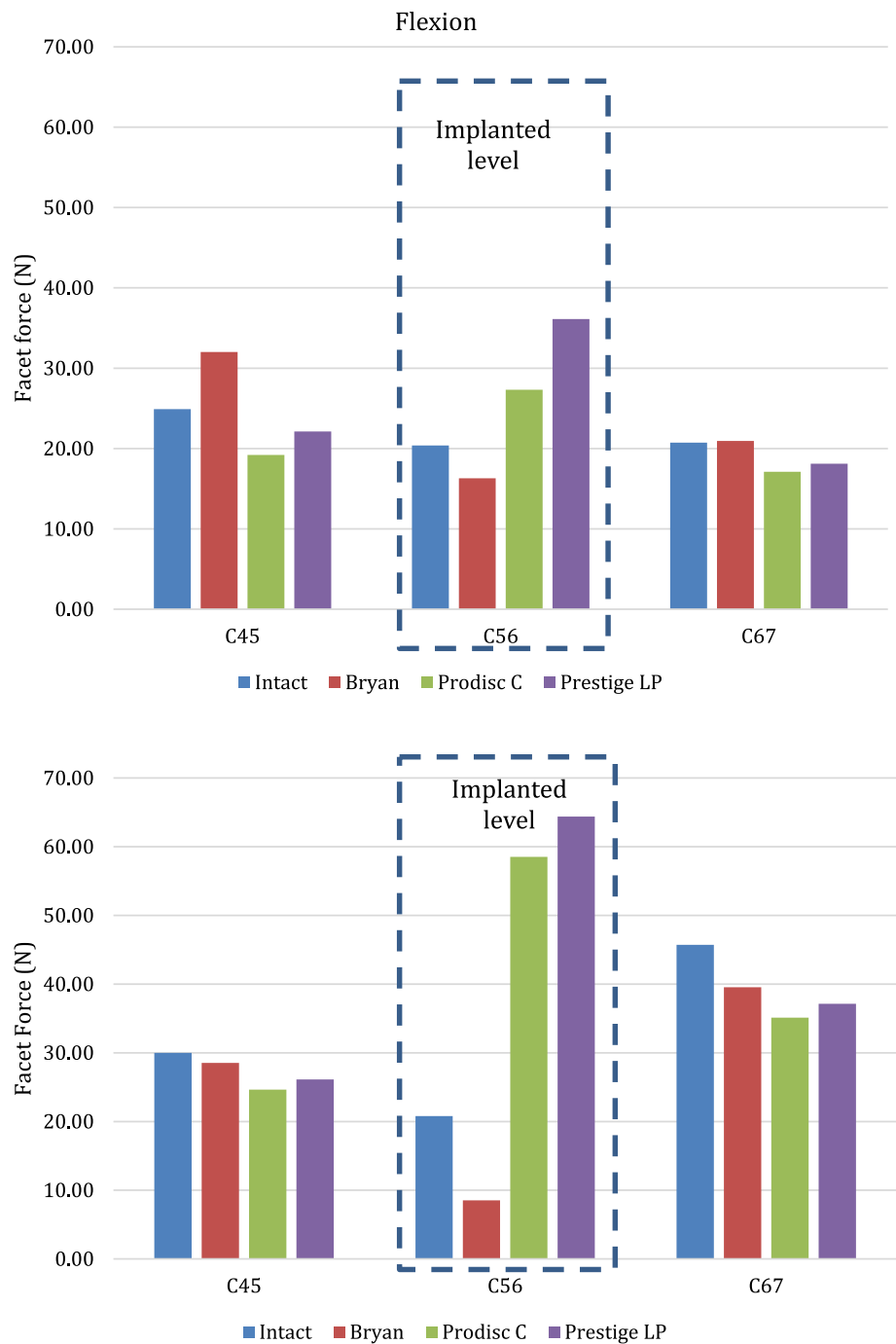
Bryan elevated intradiscal pressure (IDP) only in flexion (by 10.45% at C4/5 and 1.76% at C6/7), but decreased

Fig. 3 Range of motion

IDP in extension (by 18.65% at C4/5 and 7.25% at C6/7) (Fig. 5). Prodisc C decreased IDP at adjacent levels in both flexion and extension (by 1.95% and 5.12% at C4/5 and C6/7, respectively, in flexion; by 27.58% and 38.17% at C4/5 and C6/7, respectively, in extension). Prestige LP slightly elevated IDP at the adjacent levels (by 5.8% in flexion at C4/5 and C6/7; by 4.61% and 8.21% in extension at C4/5 and C6/7, respectively).

Discussion

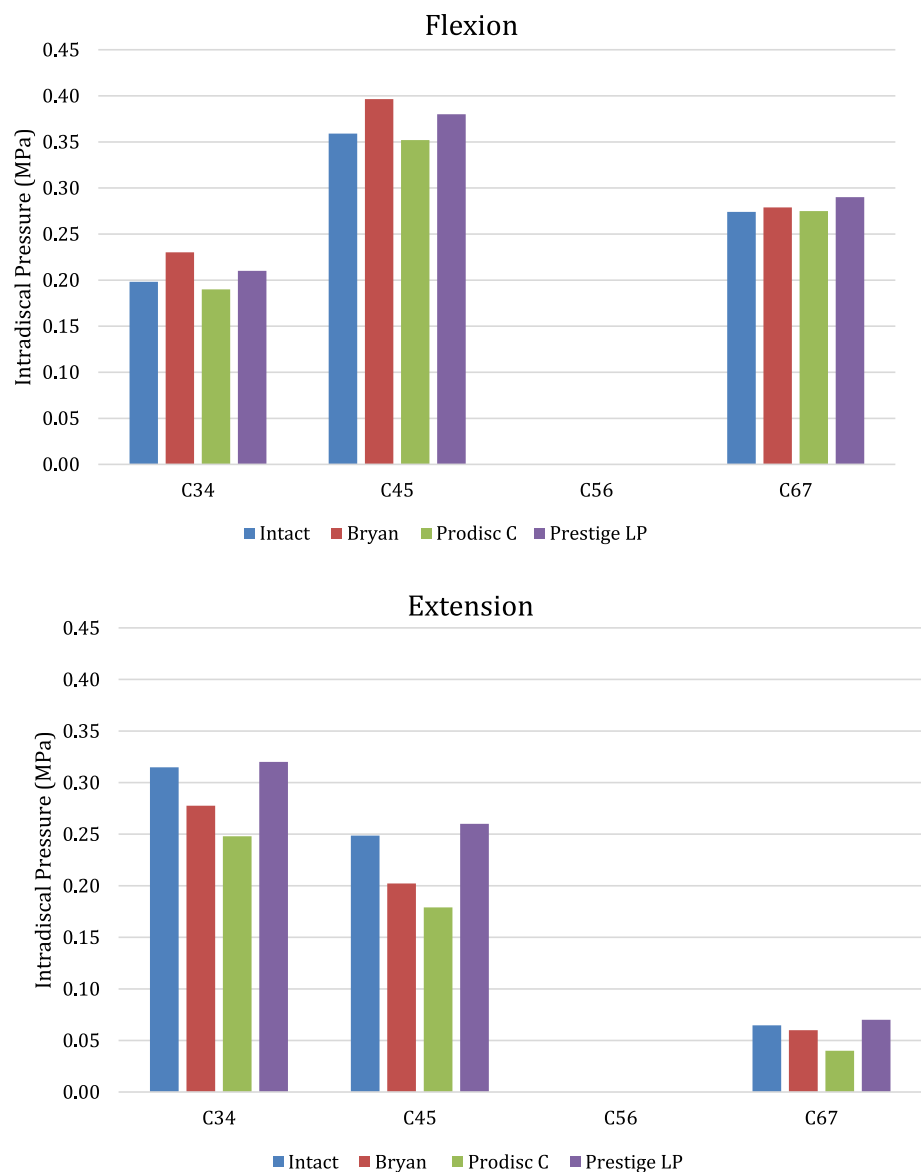
The three cervical artificial discs were chosen due to their current or previous global popularity and their representation of different design paradigms. Prestige LP is an open two-piece, semi-constrained design with metal-on-metal articulation. Prodisc C is an open two-piece, semi-constrained design with polymer-on-metal articulation. Bryan is a closed one-piece, unconstrained (no fixed core or centre of

Fig. 4 Facet force

rotation) design with a saline-lubricated polyurethane core. These varying designs resulted in different biomechanical alterations in the cervical spine after arthroplasty.

Prodisc C and Prestige LP increased motion (in flexion and extension) to a supraphysiologic range and greatly elevated the facet force at the index level. This is in concordance with the existing literature [2, 9] and the known clinical contraindications of spinal instability and facet arthropathy for cervical arthroplasty. Prodisc C and Prestige LP share an open two-piece semi-constrained design. Prestige LP has

an upside-down metal dome that articulates with a metal crater that is slightly bigger (metal-on-metal), allowing up to 2 mm in anterior/posterior translation [34]. Prodisc C has a polymer core that is attached to the inferior plate, which then articulates with the superior metal plate that acts as a socket (ball and socket; polymer-on-metal). Translation of the centre of rotation is allowed in Prodisc C only when coupled with rotation (coupled motion rotational translation). Open unconstrained designs, such as Mobi-C (Zimmer Biomet, Warsaw, IN, USA) (which allows approximately

Fig. 5 Intradiscal pressure

1 mm of lateral and anterior–posterior translation of the polymer core), may result in even higher ROM and FF at the index level. Prodisc C and Prestige LP differed in the way they changed the intradiscal pressure at the adjacent levels. The all-metal rigid construction of Prestige LP may have led to the increased IDP at the adjacent levels. In contrast, the polymer core of Prodisc C, with its lower Young's modulus, could be responsible for the reduced IDP at the adjacent levels.

The Bryan disc resulted in unique biomechanical alterations different from Prodisc C and Prestige LP. This is attributable to its encapsulated design with an unconstrained core that more closely mimics the natural disc space. Interestingly, it shielded the facets at the index level in both flexion and extension. This is likely due to limiting the range of motion at the index level to a largely physiologic range.

Gandhi also found that the Bryan model exhibited lower facet forces than the Prestige LP model [6]. However, Kang and colleagues applied 73.6 N of axial precompression rostral to the C5–6 functional spinal unit and found that the facet stress in the Bryan model reached a supraphysiologic level while Prestige LP and Prodisc C remained subphysiologic [10]. This is likely attributable to the polyurethane core in the Bryan model having a lower Young's modulus than the titanium core of Prestige LP and the UHMWPE (ultra-high molecular weight polyethylene) core of Prodisc C. Lin and colleagues showed that the material composition of the artificial discs also influences the load sharing pattern and stress concentration at the implant/bone interface [12]. These findings demonstrate that the facet stresses are determined by not only the range of motion but also the biomaterial characteristics of the artificial disc.

The Bryan disc maintained a range of motion similar to the intact spine model in extension, but exhibited diminished flexion at the index level, while increasing ROM at the adjacent levels. This correlated with increased intradiscal pressure and facet force in the adjacent levels in flexion. Galbusera and colleagues also found that the Bryan model exhibited reduced flexion compared to the intact model [5]. The Bryan disc's limitation in flexion may be due to a combination of its closed compartment design and the intact posterior ligamentous structures. Interestingly, Chen and colleagues found that the Bryan disc implanted into a kyphotic cervical spine could be exposed to increased anterior compressive loads with flexion and could lead to anterior collapse of the implant [3]. These findings demonstrate the influence of design and material composition on the behaviour of the artificial disc and the cervical spine. The minimally increased extension ROM at the index level is likely due to the removal of anterior longitudinal ligament during surgery.

There are other variables with respect to the implant and the spine that could not be simulated. For example, surgeons may size the implants differently causing varying degrees of distraction at the index level, or place them too anteriorly (for fear of spinal cord compression) or laterally (depending on the laterality of the approach and/or lack of visualization of the bilateral uncovertebral joints). Position of the centre of rotation could affect the intervertebral rotation and facet force [4]. There could be motion between the vertebral bodies and the artificial disc before osseointegration takes place. Lin and colleagues warned against the risk of subsidence with artificial discs containing keel(s) and rigid cores [12]. Particulate-induced osteolysis could loosen the implants and cause migration and/or subsidence [35]. Although flexion and extension were simulated in the study, the spine clinically undergoes complex combined movements that are difficult to replicate. Additional studies can be conducted using our model to examine some of the aforementioned variables such as implant size/placement and loading patterns. Another extension of this research would be to examine the role of disc component material properties at the adjacent levels over time. Any degenerative effect of the adjacent levels may alter internal load sharing between the disc and facets and could play an accentuated role in patients with an advanced age and/or activities that may predispose to such degenerative changes (such as in the military population) [36].

Conclusions

Design and material composition of the artificial disc have a profound impact on the biomechanical alterations at the index and adjacent levels of the cervical spine after cervical arthroplasty. Bryan, Prodisc C, and Prestige LP cervical disc replacements have unique biomechanical signatures.

Acknowledgements This material is the result of work supported by the U.S. Department of Defense, Medical Research and Materiel Command, Grant W81XWH-16-1-0010, with the resources and use of facilities at the Zablocki VA Medical Center, Milwaukee, Wisconsin, and the Center for NeuroTrauma Research (CNTR) from the Department of Neurosurgery. The last author is a part-time employee of the VA Medical Center, Milwaukee, Wisconsin. Any views expressed in this article are those of the authors and not necessarily representative of the funding organizations.

Compliance with ethical standards

Conflict of interest The authors declare that they have no conflict of interest.


References

1. Xu JC, Goel C, Shriver MF, Tanenbaum JE, Steinmetz MP, Benzel EC, Mroz TE (2018) Adverse events following cervical disc arthroplasty: a systematic review. *Glob Spine J* 8(2):178–189. <https://doi.org/10.1177/2192568217720681>
2. Chang UK, Kim DH, Lee MC, Willenberg R, Kim SH, Lim J (2007) Range of motion change after cervical arthroplasty with ProDisc-C and prestige artificial discs compared with anterior cervical discectomy and fusion. *J Neurosurg Spine* 7(1):40–46. <https://doi.org/10.3171/SPI-07/07/040>
3. Chen WM, Jin J, Park T, Ryu KS, Lee SJ (2018) Strain behavior of malaligned cervical spine implanted with metal-on-polyethylene, metal-on-metal, and elastomeric artificial disc prostheses—a finite element analysis. *Clin Biomech (Bristol, Avon)* 59:19–26. <https://doi.org/10.1016/j.clinbiomech.2018.08.005>
4. Galbusera F, Anasetti F, Bellini CM, Costa F, Fornari M (2010) The influence of the axial, antero-posterior and lateral positions of the center of rotation of a ball-and-socket disc prosthesis on the cervical spine biomechanics. *Clin Biomech (Bristol, Avon)* 25(5):397–401. <https://doi.org/10.1016/j.clinbiomech.2010.01.010>
5. Galbusera F, Fantigrossi A, Raimondi MT, Sassi M, Fornari M, Assietti R (2006) Biomechanics of the C5–C6 spinal unit before and after placement of a disc prosthesis. *Biomech Model Mechanobiol* 5(4):253–261. <https://doi.org/10.1007/s10237-006-0015-4>
6. Gandhi AA (2012) Biomechanical analysis of the cervical spine following total disc arthroplasty: an experimental and finite element investigation. University of Iowa, Iowa City
7. Gandhi AA, Kode S, DeVries NA, Grosland NM, Smucker JD, Fredericks DC (2015) Biomechanical analysis of cervical disc replacement and fusion using single level, two level, and hybrid constructs. *Spine (Phila Pa 1976)* 40(20):1578–1585. <https://doi.org/10.1097/BRS.0000000000001044>
8. Hu N, Cunningham BW, McAfee PC, Kim SW, Seftor JC, Cappuccino A, Pimenta L (2006) Porous coated motion cervical disc replacement: a biomechanical, histomorphometric, and biologic wear analysis in a caprine model. *Spine (Phila Pa 1976)* 31(15):1666–1673. <https://doi.org/10.1097/01.brs.0000224537.79234.21>
9. Jung TGW, Woo SH, Park KM, Jang JW, Han DW, Lee SJ (2013) Biomechanical behavior of two different cervical total disc replacement designs in relation of concavity of articular surfaces: prodisc-C versus prestige-LP. *Int J Precis Eng Manuf* 14(5):819–824
10. Kang H, Park P, La Marca F, Hollister SJ, Lin CY (2010) Analysis of load sharing on uncovertebral and facet joints at the C5–6 level with implantation of the Bryan, Prestige LP, or ProDisc-C cervical disc prosthesis: an in vivo image-based

- finite element study. *Neurosurg Focus* 28(6):E9. <https://doi.org/10.3171/2010.3.FOCUS1046>
11. Li Y, Zhang Z, Liao Z, Mo Z, Liu W (2017) Finite element analysis of influence of axial position of center of rotation of a cervical total disc replacement on biomechanical parameters: simulated 2-level replacement based on a validated model. *World Neurosurg* 106:932–938. <https://doi.org/10.1016/j.wneu.2017.07.079>
 12. Lin CY, Kang H, Rouleau JP, Hollister SJ, Marca FL (2009) Stress analysis of the interface between cervical vertebrae end plates and the Bryan, Prestige LP, and ProDisc-C cervical disc prostheses: an in vivo image-based finite element study. *Spine (Phila Pa 1976)* 34(15):1554–1560. <https://doi.org/10.1097/BRS.0b013e3181aa643b>
 13. Tan QC, Feng YF, Zhang Y, Wu ZX, Ma ZS, Sang HX, Yan YB, Lei W, Zhao X (2015) A novel total cervical prosthesis for single-level cervical subtotal corpectomy: radiologic and histomorphometric analysis in a caprine model. *J Spinal Disord Tech* 28(3):E166–172. <https://doi.org/10.1097/BSD.0000000000000202>
 14. Helgeson MD, Bevevino AJ, Hilibrand AS (2013) Update on the evidence for adjacent segment degeneration and disease. *Spine J* 13(3):342–351. <https://doi.org/10.1016/j.spinee.2012.12.009>
 15. Moatz B, Tortolani PJ (2012) Cervical disc arthroplasty: Pros and cons. *Surg Neurol Int* 3(Suppl 3):S216–224. <https://doi.org/10.4103/2152-7806.98582>
 16. Ren C, Song Y, Xue Y, Yang X (2014) Mid- to long-term outcomes after cervical disc arthroplasty compared with anterior discectomy and fusion: a systematic review and meta-analysis of randomized controlled trials. *Eur Spine J* 23(5):1115–1123. <https://doi.org/10.1007/s00586-014-3220-3>
 17. ASTM (2006) Standard guide for functional, kinematic, and wear assessment of total disc prostheses. ASTM F2423–05
 18. de Jongh CU, Basson AH, Scheffer C (2008) Predictive modelling of cervical disc implant wear. *J Biomech* 41(15):3177–3183. <https://doi.org/10.1016/j.jbiomech.2008.08.025>
 19. ISO (2005) Implants for surgery—wear of total intervertebral spinal disc prostheses—part 1: loading and displacement parameters for wear testing and corresponding environmental conditions for tests. ISO/DIS 18192–1
 20. Bhattacharya S, Goel VK, Liu X, Kiapour A, Serhan HA (2011) Models that incorporate spinal structures predict better wear performance of cervical artificial discs. *Spine J* 11(8):766–776. <https://doi.org/10.1016/j.spinee.2011.06.008>
 21. Yeh CH, Hung CW, Kao CH, Chao CM (2014) Medium-term outcomes of artificial disc replacement for severe cervical disc narrowing. *J Acute Dis* 3(4):290–295
 22. John JD, Saravana Kumar G, Yoganandan N (2019) Cervical spine morphology and ligament property variations: a finite element study of their influence on sagittal bending characteristics. *J Biomech* 85:18–26. <https://doi.org/10.1016/j.jbiomech.2018.12.044>
 23. Arun MW, Yoganandan N, Stemper BD, Zheng M, Masoudi A, Snyder B (2014) Sensitivity and stability analysis of a nonlinear material model of cervical intervertebral disc under cyclic loads using the finite element method. *Biomed Sci Instrum* 50:19–30
 24. Wheelodon JA, Stemper BD, Yoganandan N, Pintar FA (2008) Validation of a finite element model of the young normal lower cervical spine. *Ann Biomed Eng* 36(9):1458–1469. <https://doi.org/10.1007/s10439-008-9534-8>
 25. Wheelodon JA, Pintar FA, Knowles S, Yoganandan N (2006) Experimental flexion/extension data corridors for validation of finite element models of the young, normal cervical spine. *J Biomech* 39(2):375–380. <https://doi.org/10.1016/j.jbiomech.2004.11.014>
 26. Bell KM, Yan Y, Hartman RA, Lee JY (2018) Influence of follower load application on moment-rotation parameters and intradiscal pressure in the cervical spine. *J Biomech* 76:167–172. <https://doi.org/10.1016/j.jbiomech.2018.05.031>
 27. Patel VV, Wuthrich ZR, McGilvray KC, Laffleur MC, Lindley EM, Sun D, Puttlitz CM (2017) Cervical facet force analysis after disc replacement versus fusion. *Clin Biomech (Bristol, Avon)* 44:52–58. <https://doi.org/10.1016/j.clinbiomech.2017.03.007>
 28. Wang Z, Zhao H, Liu JM, Tan LW, Liu P, Zhao JH (2016) Resection or degeneration of uncovertebral joints altered the segmental kinematics and load-sharing pattern of subaxial cervical spine: A biomechanical investigation using a C2–T1 finite element model. *J Biomech* 49(13):2854–2862. <https://doi.org/10.1016/j.jbiomech.2016.06.027>
 29. Mercer S, Bogduk N (1999) The ligaments and annulus fibrosus of human adult cervical intervertebral discs. *Spine (Phila Pa 1976)* 24(7):619–626; discussion 627–618
 30. Kumaresan S, Yoganandan N, Pintar FA, Macias M, Cusick JF (2000) Morphology of young and old cervical spine intervertebral disc tissues. *Biomed Sci Instrum* 36:141–146
 31. Kumaresan S, Yoganandan N, Pintar FA, Maiman DJ (1999) Finite element modeling of the cervical spine: role of intervertebral disc under axial and eccentric loads. *Med Eng Phys* 21(10):689–700
 32. Panjabi MM (2007) Hybrid multidirectional test method to evaluate spinal adjacent-level effects. *Clin Biomech (Bristol, Avon)* 22(3):257–265. <https://doi.org/10.1016/j.clinbiomech.2006.08.006>
 33. Liao Z, Fogel GR, Wei N, Gu H, Liu W (2015) Biomechanics of artificial disc replacements adjacent to a 2-level fusion in 4-level hybrid constructs: an in vitro investigation. *Med Sci Monit* 21:4006–4014
 34. Choi H, Baisden JL, Yoganandan N (2019) A Comparative in vivo study of semi-constrained and unconstrained cervical artificial disc prostheses. *Mil Med* 184(Suppl 1):637–643. <https://doi.org/10.1093/milmed/usy395>
 35. Hacker FM, Babcock RM, Hacker RJ (2013) Very late complications of cervical arthroplasty: results of 2 controlled randomized prospective studies from a single investigator site. *Spine (Phila Pa 1976)* 38(26):2223–2226. <https://doi.org/10.1097/BRS.0000000000000060>
 36. Byeon JH, Kim JW, Jeong HJ, Sim YJ, Kim DK, Choi JK, Im HJ, Kim GC (2013) Degenerative changes of spine in helicopter pilots. *Ann Rehabil Med* 37(5):706–712. <https://doi.org/10.5535/arm.2013.37.5.706>

Publisher's Note Springer Nature remains neutral with regard to jurisdictional claims in published maps and institutional affiliations.

Affiliations

Hoon Choi¹  · Yuvaraj Purushothaman^{1,2} · Jamie Baisden¹ · Narayan Yoganandan¹

¹ Department of Neurosurgery, Medical College of Wisconsin, HUB, 8701, Watertown Plank Road, Milwaukee, WI, USA

² School of Mechanical and Building Science, VIT University, Chennai Campus, Chennai, India